Orbital Clinicopathological Differences in Thyroid Eye Disease: An Analysis of Cytokines With Histopathological and Clinical Correlation

Yue Li,[1,2] Jiaqi Tang,[1,2] Gaojing Jing,[2,3] Yueyue Li,[2] Rui Ma,[2] Xin Kang,[2] Liyuan Rong,[2,4] Wenlu Liu,[2] Lan Yao,[2] Xiaohui Lv,[1] Aijun Deng,[1] Wei Wu,[2] and Xinji Yang[1,2]

[1]School of Clinical Medicine, Shandong Second Medical University, Weifang, Shandong, China
[2]Senior Department of Ophthalmology, 3rd Medical Center of Chinese PLA General Hospital, Beijing, China
[3]Department of Endocrinology, The First Hospital of Lanzhou University, Lanzhou, Gansu, China
[4]Stem Cell and Regenerative Medicine Lab, Beijing Institute of Radiation Medicine, Beijing, China

Correspondence: Wei Wu, Senior Department of Ophthalmology, 3rd Medical Center of Chinese PLA General Hospital, No. 69 Yongding Rd., Haidian District, Beijing 100143, China; wuwei1@301hospital.com.cn. Xinji Yang, Senior Department of Ophthalmology, 3rd Medical Center of Chinese PLA General Hospital, No. 69 Yongding Rd., Haidian District, Beijing 100143, China; yangxinji68@sina.com.

Received: October 26, 2024
Accepted: February 5, 2025
Published: March 18, 2025

Citation: Li Y, Tang J, Jing G, et al. Orbital clinicopathological differences in thyroid eye disease: An analysis of cytokines with histopathological and clinical correlation. *Invest Ophthalmol Vis Sci.* 2025;66(3):33. https://doi.org/10.1167/iovs.66.3.33

Purpose. To explore the pathological differences in orbital adipose/connective tissue between active and inactive thyroid eye disease (TED) subjects and their correlations with clinical characteristics.

Methods. Orbital adipose/connective tissue samples from 42 TED subjects (20 active, 22 inactive) were collected during decompression surgery. We analyzed cytokine expression, inflammatory cell infiltration, inherent cell populations, and interstitial changes by Luminex and histopathology. Correlations were analyzed using Pearson and Spearman correlation analyses.

Results. Among the 108 cytokines detected, active TED exhibited elevated platelet endothelial cell adhesion molecule 1 (PECAM-1), interleukin-23 (IL-23), a proliferation-inducing ligand (APRIL), IL-6, C-C motif chemokine ligand 2 (CCL2), β-nerve growth factor (NGF), and lower CCL21 and CCL5. The extent of infiltration by helper T (Th) cells and monocytes was significantly greater in the active group than in the inactive group. Adipocyte density was significantly elevated in active TED, whereas fibrosis was more prominent in inactive TED. Fifteen cytokines were significantly associated with inflammatory cell infiltration, with IL-16 showing the strongest correlations with T cells. Ten cytokines showed significant positive correlations with fibrosis. Four cytokines (IL-6, PECAM-1, IL-23 and transforming growth factor β1), Th cell infiltration and adipocyte density were significantly positively correlated with clinical activity score (CAS). Sixteen cytokines, along with adipocyte density, were significantly positively correlated with disease severity of TED.

Conclusions. The orbital adipose/connective tissues of active and inactive TED subjects showed significant differences in terms of cytokines, inflammatory cells infiltration, inherent cells and interstitium. These pathological changes were correlated with clinical characteristics of TED.

Keywords: thyroid eye disease, cytokines, pathological differences, clinicopathological correlation, targeted therapy

Thyroid eye disease (TED) is a kind of organ-specific autoimmune orbital disease usually associated with thyroid disorders. This complex disease potentially alters the appearance of patients and threatens the vision, which seriously impedes the quality of individuals' lives.[1,2] The major pathological changes of TED are characterized by chronic multifactorial inflammation, which leads to histopathological alterations, including inflammatory cell infiltration, fibroblast activation, adipogenesis, glycosaminoglycan accumulation, and fibrosis in the orbital adipose/connective tissue.[3–5] In addition, a variety of cytokines are considered to play an important role in the pathogenesis of TED.[6]

Inevitably, different states of inflammation result in varied clinical manifestations in TED patients. Symptoms such as pain, congestion, and edema are often associated with inflammation, which are signs of disease activity. Clinically, TED activity is often graded by the CAS, which classifies patients as active or inactive based on these inflammatory-related clinical symptoms. The specific assessment of CAS includes seven criteria: spontaneous orbital pain, gaze-evoked orbital pain, eyelid erythema, eyelid edema, conjunctival redness, chemosis, and caruncle edema.[7] However, the pathological differences at the cellular or even molecular levels between active and inactive TED patients remain unclear. Addressing this issue is critical, not only to facilitate the accurate diagnosis and treatment of TED, but also to lay a crucial foundation for clarifying the relationship between the clin-

ical manifestations and the pathological alterations of TED.

Currently, several studies have reported the pathological differences of orbital adipose/connective tissue between active and inactive TED patients from different perspectives. A previous study has reported that infiltration of inflammatory B and T lymphocytes in the orbital tissue of TED patients is significantly correlated with disease activity.[8] Besides, in comparison to inactive TED patients, the density of neovasculature and lymphatic vessels, as well as the expression of proinflammatory cytokines IL-1, IL-6, IL-8, and IL-10, were significantly increased in orbital adipose/connective tissue of active TED patients.[9,10] However, these investigations are constrained by several limitations, including narrow detection contents, limited detection indicators, and low-throughput detection strategies. Therefore a comprehensive and deep understanding of the histopathologic differences between active and inactive TED patients is important.

In this study, we adopted a high-throughput approach to detect the differential expression of multiplex cytokines in orbital adipose/connective tissue between active and inactive TED subjects. Additionally, a comprehensive histopathological analysis was then performed to evaluate the pathological differences of inflammatory cell infiltration, inherent cells and interstitium in orbital adipose/connective tissue between the two groups. We further investigated the correlations between the above pathological changes and the clinical manifestations, including CAS, severity, exophthalmos, and diplopia in TED subjects. These findings had the potential to provide a foundation for the precise diagnosis and treatment of TED.

Method

Statements on Compliance With Ethical Standards

The study followed the Helsinki Declaration and was approved by the regional research ethics committee of the Senior Department of Ophthalmology, the Third Medical Center, Chinese People's Liberation Army (PLA) General Hospital (project number KY2024-002). All participating subjects have signed the informed consent following the comprehensive explanations of the study's purpose and the nature of all procedures involved.

Participants

This study includes TED subjects who underwent orbital decompression surgery between December 2022 and December 2023 at the Senior Department of Ophthalmology, the Third Medical Center, Chinese PLA General Hospital. The diagnosis of TED was established according to Bartley's criteria.[11]

The exclusion criteria encompassed TED subjects with a documented history of steroid therapy (including local injections, oral or intravenous administration) or immunosuppressive treatment within past three months. Additionally, individuals with other autoimmune diseases, malignancies, or severe infectious conditions were also excluded. A total of 42 TED subjects were ultimately enrolled in the study. The inflammation activity of the disease was assessed using CAS.[2] TED subjects with CAS $\geq$ 3/7 were divided into the active group (n = 20, 20 eyes) and those with CAS $<$ 3/7 into the inactive group (n = 22, 22 eyes). The severity of the disease was classified in accordance with the 2021 guidelines of the European Group on Graves' Orbitopathy,[2] which categorizes TED into mild, moderate-to-severe, and sight-threatening stages.

Ocular Examinations

The assessment of TED was performed by the same two ophthalmologists according to standardized clinical protocols. Exophthalmos was measured using the Hertel exophthalmometer with a threshold significantly more than 16 mm, defining proptosis.[12,13] Diplopia was assessed based on the Gorman diplopia score.[14]

Multiplex Analysis of Cytokines With Luminex Assays

All the orbital adipose/connective tissues were collected during orbital decompression surgery. First, 10 mg of each tissue was mixed with 200-300 µL of lysis buffer containing 150 mM NaCl, 20 mM Tris-Cl, 1 mM EDTA, 1 mM EGTA, and 1% Triton-X-100. The tissue was homogenized using a tissue homogenizer. The mixture was then incubated at 4°C for 20 minutes, followed by centrifugation at 13,000 rpm for 10 minutes at 4°C. The supernatant obtained was subjected to bicinchoninic acid assay for protein quantification. Multiplex panels were used to quantify the relative protein levels of cytokines. Specifically, multiplex assays were used to detect a custom array of 108 cytokines (Human TIMP Magnetic Luminex Assay, Human, catalog numbers: FCSTM18B-39, LXSAHM-30, LXSAHM-18, LXSAHM-09, FCSTM17-03, LXSAHM-08; R&D Systems, Minneapolis, MN, USA). Supplementary Table S1 provides a detailed list of the cytokines detected by each multiplex panel. The interleukin family includes the following: IL-1α, IL-1β, IL-1ra, IL-2, IL-3, IL-4, IL-5, IL-6, IL-7, IL-8, IL-9, IL-10, IL-11, IL-12p70, IL-13, IL-15, IL-16, IL-17, IL-17C, IL-17E, IL-18, IL-19, IL-21, IL-23, IL-27, IL-28A, IL-28B, IL-31, IL-33, IL-34, and IL-36β. The chemokine family includes CCL1, CCL2, CCL3, CCL4, CCL5, CCL7, CCL8, CCL11, CCL13, CCL14, CCL17, CCL18, CCL19, CCL20, CCL21, CCL22, CCL23, CCL24, CCL25, CCL26, CCL27, CCL28, C-X-C motif chemokine ligand 1 (CXCL1), CXCL2, CXCL4, CXCL5, CXCL6, CXCL7, CXCL9, CXCL10, CXCL11, CXCL13, CXCL14, CXCL16, CX3CL1, and X-C motif chemokine ligand 1 (XCL1). The growth factor family includes platelet-derived growth factor-AA (PDGF-AA), PDGF-AB, PDGF-BB, PDGF-CC, PDGF-DD, bone morphogenetic protein 2 (BMP-2), BMP-4, BMP-7, BMP-9, BMP-10, basic fibroblast growth factor (bFGF), FGF-1, FGF-13, FGF-23, transforming growth factor α (TGF-α), TGF-β1, TGF-β2, TGF-β3, hepatocyte growth factor (HGF), epidermal growth factor (EGF), vascular endothelial growth factor (VEGF), heparin-binding EGF (HB-EGF), and placental growth factor (PGF). Other cytokines include: granulocyte colony-stimulating factor (G-CSF), granulocyte-macrophage CSF (GM-CSF), intercellular adhesion molecule-1 (ICAM-1), vascular cell adhesion molecule-1 (VCAM-1), PECAM-1, β-NGF, brain-derived neurotrophic factor (BDNF), APRIL, neurotrophin-3 (NT-3), NT-4, tumor necrosis factor-α (TNF-α), TNF-related activation-inducer (TRANCE), interferon-γ (IFN-γ), serpin family E member 1 (SERPINE1), CD40 ligand, thrombopoietin, leptin, and adiponectin.

Investigative Ophthalmology & Visual Science

Immunohistochemical and Histological Staining Analysis

Among the 42 enrolled subjects, adequate orbital adipose connective tissue specimens were obtained from 33 subjects (18 with active TED and 15 with inactive TED). Consequently, paraffin-embedded orbital adipose/connective tissue samples were successfully acquired from these 33 subjects for further histopathological analysis. The paraffin sections were subjected to routine histological staining, including hematoxylin and eosin (H&E) (Service Bio, Wuhan, China), Masson's trichrome stain (Service Bio), and Alcian blue (Service Bio).

We detected the expressions of CD3, CD4, CD8, CD14, CD19 and CD90 by immunohistochemistry. In brief, the paraffin sections were deparaffinized in dewaxing solution (Service Bio) and rehydrated in graded alcohols (Sinopharm, Shanghai, China). Antigen retrieval was then performed by immersing the sections in 20 × Tris-EDTA solution. Endogenous peroxidase was quenched with 3% hydrogen peroxide (Annjet, Shandong, China) in methanol. Nonspecific protein-binding sites were blocked with serum or BSA for 30 minutes. Next, the sections were incubated with primary antibodies (listed in Supplementary Table S2) overnight at 4 °C. On the following day, the slides were washed with PBS and then incubated with the corresponding species-specific secondary antibody (HRP-marked) at room temperature for 50 minutes. Chromogen detection was performed using diaminobenzidine (Service Bio), followed by counterstaining with hematoxylin (Service Bio). The nuclei stained with hematoxylin appeared blue, while positive diaminobenzidine signals were brownish-yellow.

Quantitative Histopathological Evaluation

The immunohistochemical tissue sections were scanned using the Pannoramic MIDI (3DHISTECH Ltd, Budapest, Hungary) and automatically measured using Augathella image analysis software (Service Bio). We quantitatively calculated the positive area ratio by dividing the positive cell area by the area of the tissue slice.

For the quantitative analysis of H&E, Masson, and Alcian blue staining, three images were randomly taken from three different fields of each slide using an Eclipse Ci-L microscope (Nikon Inc., Melville, NY, USA). Image-Pro Plus 6.0 software (IBM Corp., Armonk, NY, USA) was used to quantify the number of adipocytes per field after H&E staining. Adipocyte density was expressed as the number of adipocytes per square millimeter.

Masson's trichrome staining was used to differentiate three primary pathological components: muscle (red), fibrosis (blue), and adipose (white) under standard light microscopy. Blue staining was designated as Masson-positive and automatically measured using Augathella image analysis software (Service Bio).[15] The extent of fibrosis was expressed as the ratio of the Masson-positive area to the image area.

In the analysis of Alcian blue-stained sections, the pixel area served as the standard unit for quantifying both the positive pixel area and the total tissue pixel area. The percentage of Alcian blue-positive area, calculated as the ratio of positive pixel area to total tissue pixel area using Augathella image analysis software (Service Bio), was used to represent the glycosaminoglycan staining results.

Statistical Analysis

Statistical analysis was performed using SPSS 29.0 (IBM Corp.). Data were plotted with GraphPad Prism 9.0 (GraphPad Software, San Diego, CA, USA). The variables were first checked for normality using the Shapiro-Wilk test. The *t*-test or Mann-Whitney U test was adopted to make comparisons between the two groups. Continuous variables were presented as mean ± standard deviation (SD) or median (25th percentile and 75th percentile), depending on their distribution. The Pearson correlation was used to analyze the relationship between two continuous variables. The Spearman correlation was used to analyze the relationship between continuous and ordinal variables. $P \leq 0.05$ was considered statistically significant.

Results

Differential Concentrations of 106 Cytokines in Orbital Adipose/Connective Tissue Between Active and Inactive TED Subjects

To examine the pathological differences of orbital adipose/connective tissue between active and inactive TED, we recruited a cohort study comprising 20 active TED individuals and 22 inactive TED individuals. All participants underwent orbital decompression surgery, which allowed the collection of orbital adipose/connective tissue samples. Notably, none of the TED subjects received immunosuppressive treatment within the three months preceding the surgery. Furthermore, no statistically significant difference was observed between the two groups in terms of gender, age, disease duration, thyroid function, or blood lipid (Supplementary Table S3). This high homogeneity established a robust basis for the subsequent analysis of the differences in the pathological indicators between the two groups.

We used high-throughput Luminex technology to successfully quantify the concentrations of 106 of 108 cytokines in the collected orbital adipose/connective tissue. Compared with the inactive group, the concentration levels of PECAM-1, IL-23, APRIL, IL-6, CCL2, and β-NGF in the active group were significantly increased, whereas the levels of CCL21 and CCL5 were significantly decreased (Fig. 1). Notably, the difference in concentration level of PECAM-1 was the highest between the two groups ($P = 0.008$, Fig. 1A).

Active TED Subjects Exhibited More Extended Th Cells and Monocytes Infiltration in Orbital Adipose/Connective Tissue

To further investigate the differences of inflammatory cell infiltration in orbital adipose/connective tissue between the two groups of TED subjects, immunohistochemical staining was performed on the paraffin-embedded tissue sections from 33 subjects (18 active individuals and 15 inactive individuals, Fig. 2A). We conducted a quantitative analysis to determine the density and area ratio of positive cells for CD4, CD14, CD3, CD8, and CD19 markers, which correspond to the number and extent of various inflammatory cells infiltration, respectively. The findings indicated that the mean number of inflammatory cells infiltration was greater in the active group compared to the inactive group (Supplementary Fig. S1). However, because of a substantial standard deviation, this difference was not statistically significant (Supple-

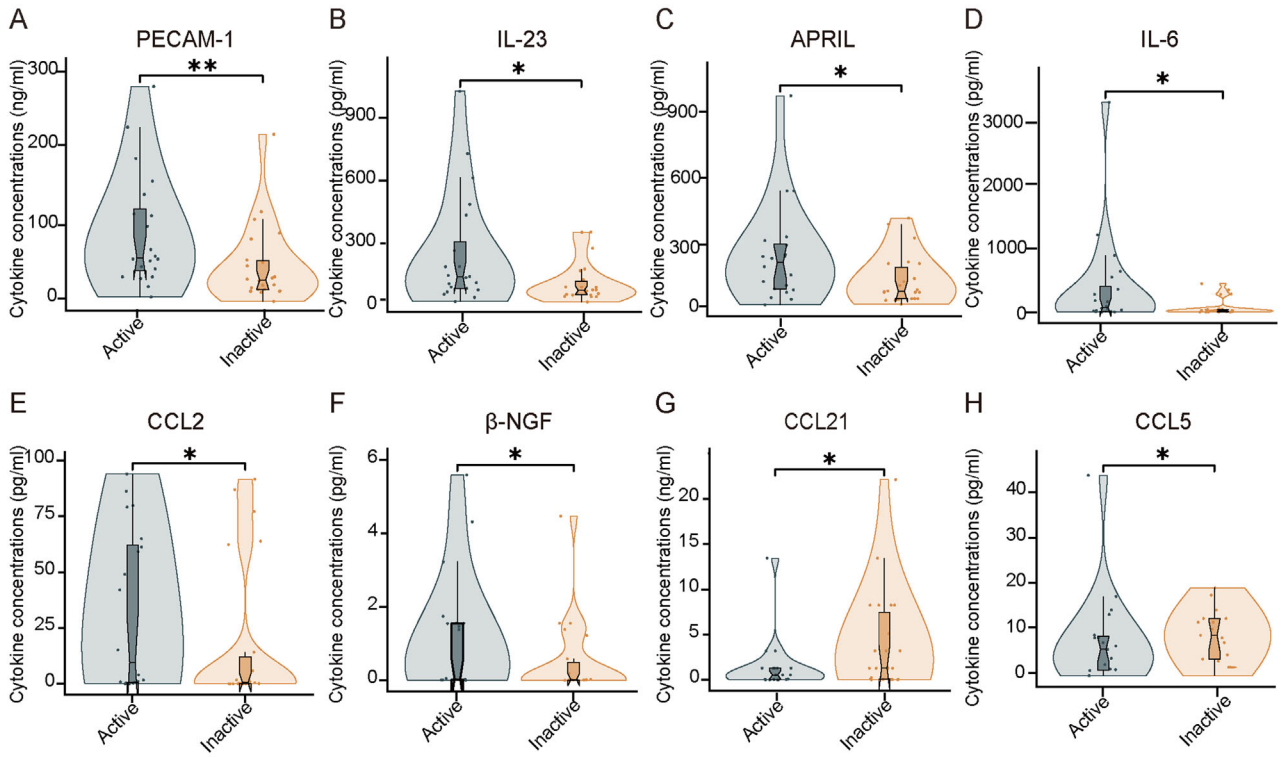

Figure 1. Cytokines with statistical difference in orbital adipose/connective tissue between active and inactive TED subjects. **(A–F)** Statistical violin plots of significantly increased cytokine concentrations in active TED subjects compared to inactive TED subjects, including **(A)** PECAM (67511.50 [46005.50, 140321.50] vs. 39609.50 [27377.50, 71127.75]; P < 0.01). **(B)** IL-23 (140.52 [81.19, 392.94] vs. 76.82 [54.11, 138.44]; P < 0.05). **(C)** APRIL (218.89 [96.94, 312.87] vs. 89.34 [56.19, 214.37]; P < 0.05). **(D)** IL-6 (77.23 [12.49, 500.39] vs. 27.43 [5.43, 48.93]; P < 0.05). **(E)** CCL2 (62.72 [21.18, 194.86] vs. 23.37 [14.85, 40.53]; P < 0.05). **(F)** β-NGF (0.04 [0.01, 1.55] vs. 0.02 [0.01, 0.75]; P < 0.05). **(G, H)** Statistical violin plots of significantly decreased cytokine concentrations in active TED subjects compared to inactive TED subjects, including **(G)** CCL21 (545.81 [50.87, 1301.00] vs. 1301.00 [77.03, 8258.00]; P < 0.05) and **(H)** CCL5 (611.04 [119.30, 1222.35] vs. 1164.00 [432.65, 7556.25]; P < 0.05). Data were presented as the median (25th percentile and 75th percentile). * $P < 0.05$; ** $P < 0.01$. ($n = 20$ in active group and $n = 22$ in inactive group.)

mentary Fig. S1). Notably, the extent of infiltration by Th cells (CD4 positive) and monocytes (CD14 positive) was significantly greater in the active group than in the inactive group (Figs. 2B, 2C). In contrast, the infiltration extents of T cells (CD3 positive), Tc cells (CD8 positive), and B cells (CD19 positive) did not differ significantly between the two groups (Figs. 2D–F).

Active TED Subjects Displayed More Adipocytes in Orbital Adipose/Connective Tissue

We further compared the differences of inherent cells in orbital adipose/connective tissue between active and inactive TED subjects, including adipocytes and fibroblasts. H&E results showed that adipocyte density in the active TED group was significantly higher compared to that in the inactive group ($P = 0.014$, Figs. 3A–C). Conversely, immunohistochemical analysis indicated no significant difference in the fibroblasts, as identified by CD90 positive area ratio, between the two groups ($P = 0.849$, Figs. 3D–F).

Inactive TED Subjects Displayed More Severe Fibrosis in Orbital Adipose/Connective Tissue

We also compared the differences in orbital adipose tissue interstitium between active and inactive subjects. Masson's trichrome staining revealed a statistically significant increase in fibrosis in the adipose/connective tissue of inactive TED subjects compared to active TED subjects ($P = 0.002$, Figs. 4A–C). However, the glycosaminoglycan content, as determined by Alcian blue staining, showed no significant difference between the two groups ($P = 0.265$, Figs. 4D–F).

Cytokines Were Closely Associated With Histopathological Changes in Orbital Adipose/Connective Tissue of TED Subjects

We further conducted a Pearson correlation analysis to explore the association between cytokine levels and the histopathological alterations in orbital adipose/connective tissue in TED subjects. The analysis included 106 cytokines and various histopathological indicators, such as inflammatory cell infiltration and adipocyte density. Results revealed that 15 cytokines were significantly associated with inflammatory cell infiltration, with IL-16 showing correlations of 0.799 with T cells, 0.693 with Tc cells, and 0.454 with Th cells (Table 1). CCL18 had the strongest correlation with Th cells ($r = 0.471$). Additionally, 11 cytokines were significantly associated with monocyte infiltration (Table 1). CXCL4 was the only cytokine significantly positively correlated with adipocyte density ($r = 0.415$). Ten cytokines showed significant positive correlations with fibrosis, with FGF-13

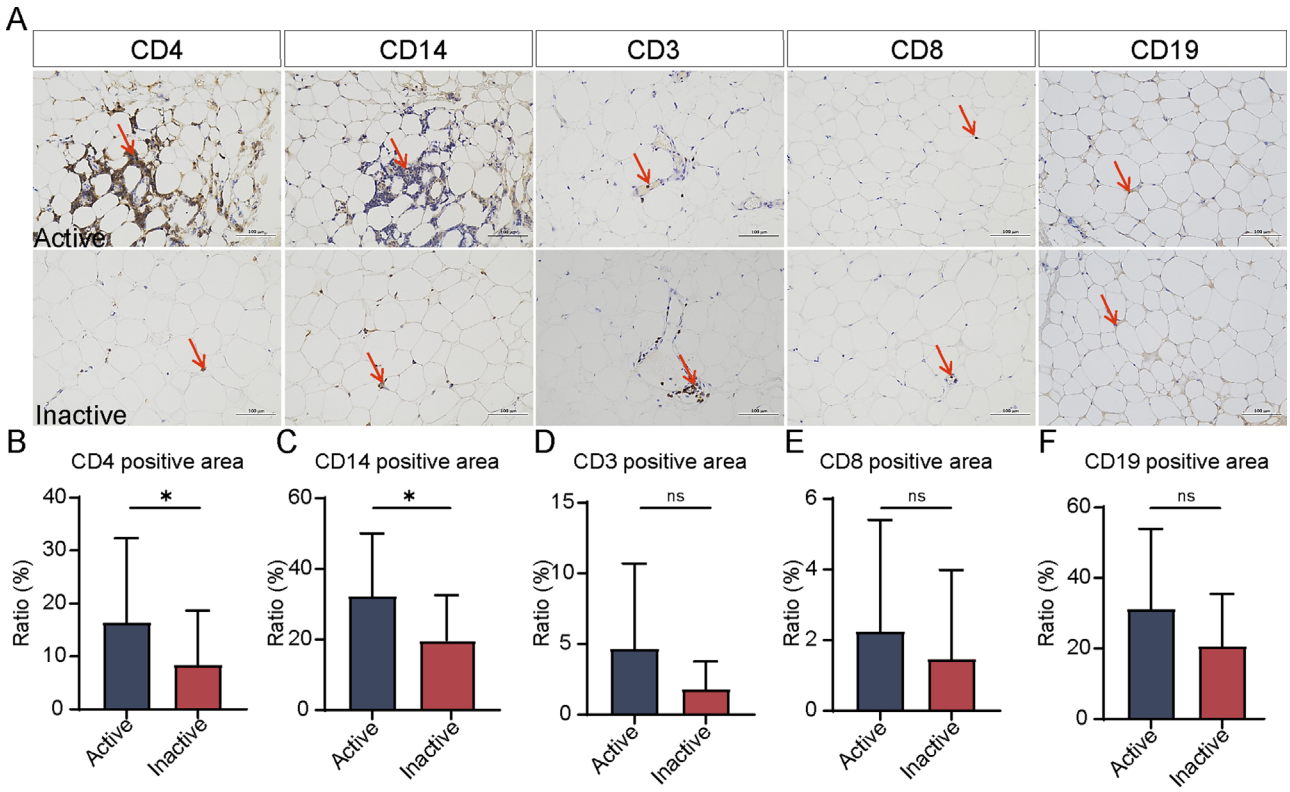

Figure 2. Differences in inflammatory cell infiltration in orbital adipose/connective tissue between active and inactive TED subjects. **(A)** Representative immunohistochemical images of CD4, CD14, CD3, CD8, and CD19 in orbital adipose/connective tissue of active and inactive TED subjects. Red arrows indicate immunohistochemically positive cells. **(B–F)** Statistical histograms of the positive area ratios for CD4 (8.71 [4.19, 26.28] vs. 4.34 [2.52, 10.62]; $P < 0.05$) **(B)**, CD14 (36.06 [13.11, 49.78] vs. 14.78 [11.88, 10.62]; $P < 0.05$) **(C)**, CD3 (1.74 [1.07, 6.53] vs. 0.91 [0.64, 1.95]; $P > 0.05$) **(D)**, CD8 (1.02 [0.66, 2.29] vs. 0.79 [0.49, 1.07]; $P > 0.05$) **(E)**, and CD19 (23.70 [12.57, 55.44] vs. 16.01 [11.95, 26.13]; $P > 0.05$) **(F)** between active and inactive groups. Data are presented as the median (25th percentile, 75th percentile). * $P < 0.05$. ns: no significant difference. ($n = 18$ in active group and $n = 15$ in inactive group.)

having the strongest correlation ($r = 0.460$). VCAM-1 was the only cytokine significantly positively correlated with glycosaminoglycan deposition ($r = 0.373$).

Cytokines and Histopathological Changes in Orbital Adipose/Connective Tissue Were Significantly Associated With Clinical Characteristics of TED Subjects

We further analyzed the correlation between all above pathological changes and clinical characteristics, such as CAS, exophthalmos, diplopia and disease severity, using Spearman rank correlation analysis. The analysis revealed that among the 106 cytokines, only IL-6, PECAM-1, IL-23, and TGF-β1 demonstrated a statistically significant positive correlation with CAS (Fig. 5A). In addition, both Th cell infiltration and adipocyte density were significantly positively correlated with CAS (Fig. 5A). Regarding exophthalmos, CXCL2 showed a significant positive correlation ($r = 0.377$), whereas CXCL11 displayed a significant negative correlation ($r = -0.308$, Fig. 5B). Furthermore, TGF-β3 and CCL5 were significantly positively correlated with diplopia (Fig. 5C). Additionally, sixteen cytokines, along with adipocyte density, were significantly positively correlated with disease severity (Table 2). The five cytokines with the strongest correlations were VCAM-1 ($r = 0.405$), CXCL5 ($r = 0.401$), CXCL13 ($r = 0.389$), APRIL ($r = 0.389$), and IL-23 ($r = 0.379$).

Discussion

It is important to elucidate the pathological distinctions in orbital adipose/connective tissue between active and inactive TED subjects. In this study, we conducted a comprehensive comparison of these pathological differences, focusing on four aspects: cytokines, infiltration of inflammatory cells, inherent cell populations, and interstitial changes.

The Luminex multiplex assay enables high-throughput quantitative detection of cytokines using microsamples with similar accuracy as the ELISA, a gold standard method for protein quantification.[16,17] Consequently, we used this Luminex multiplex assay to detect the concentrations of 108 cytokines in the orbital adipose/connective tissue. For the first time, our study identified significantly different concentrations of eight cytokines—PECAM-1, IL-23, IL-6, APRIL, CCL2, β-NGF, CCL5, and CCL21—between active and inactive TED subjects. In addition, our study, together with previous researches, has demonstrated in orbital adipose/connective tissue that active TED subjects are characterized by more severe infiltration of lymphocytes and monocytes.[8,18,19]

Regarding inherent cells, our research revealed that, for the first time, adipocyte density in the active TED group was significantly higher compared to that in the inactive group, while there was no significant difference in the number of fibroblasts between the two groups. Consistently, previous studies have demonstrated that the adipocytes in TED subjects are larger in density when compared to healthy indi-

Investigative Ophthalmology & Visual Science

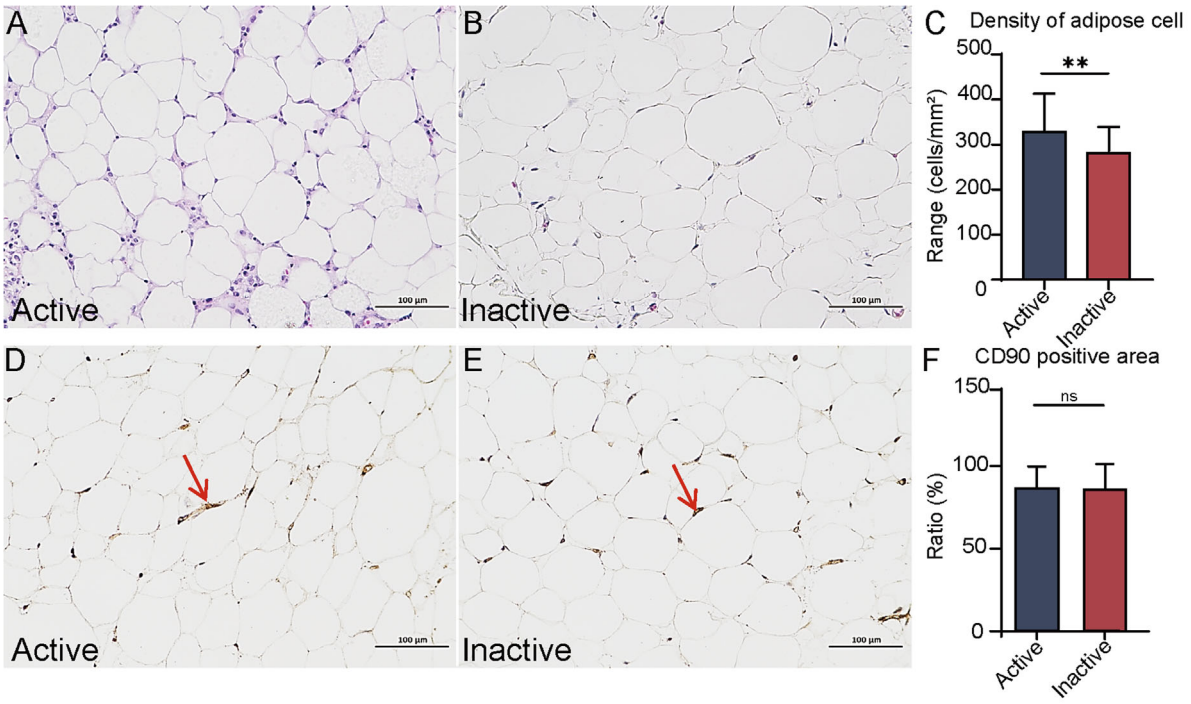

Figure 3. Differences in inherent cells of orbital adipose/connective tissue between active and inactive TED subjects. **(A–B)** Representative H&E staining images of orbital adipose/connective tissue collected from **(A)** active TED subjects and **(B)** inactive TED subjects, respectively. **(C)** The corresponding quantitative histogram of adipocyte density between two groups (0.0032 ± 0.0008 vs. 0.0036 ± 0.0007; $P < 0.01$). **(D–E)** Representative CD90 immunohistochemical staining images of orbital adipose/connective tissue in **(D)** active TED subjects and **(E)** inactive TED subjects. **(F)** The relevant quantitative histogram of CD90 positive area ratio between two groups. (86.9265 ± 12.8394 vs. 86.3938 ± 14.9231; $P > 0.05$). Data were presented as the mean ± SD. ** $P < 0.01$. ns: no significant difference. ($n = 18$ in active group and $n = 15$ in inactive group.)

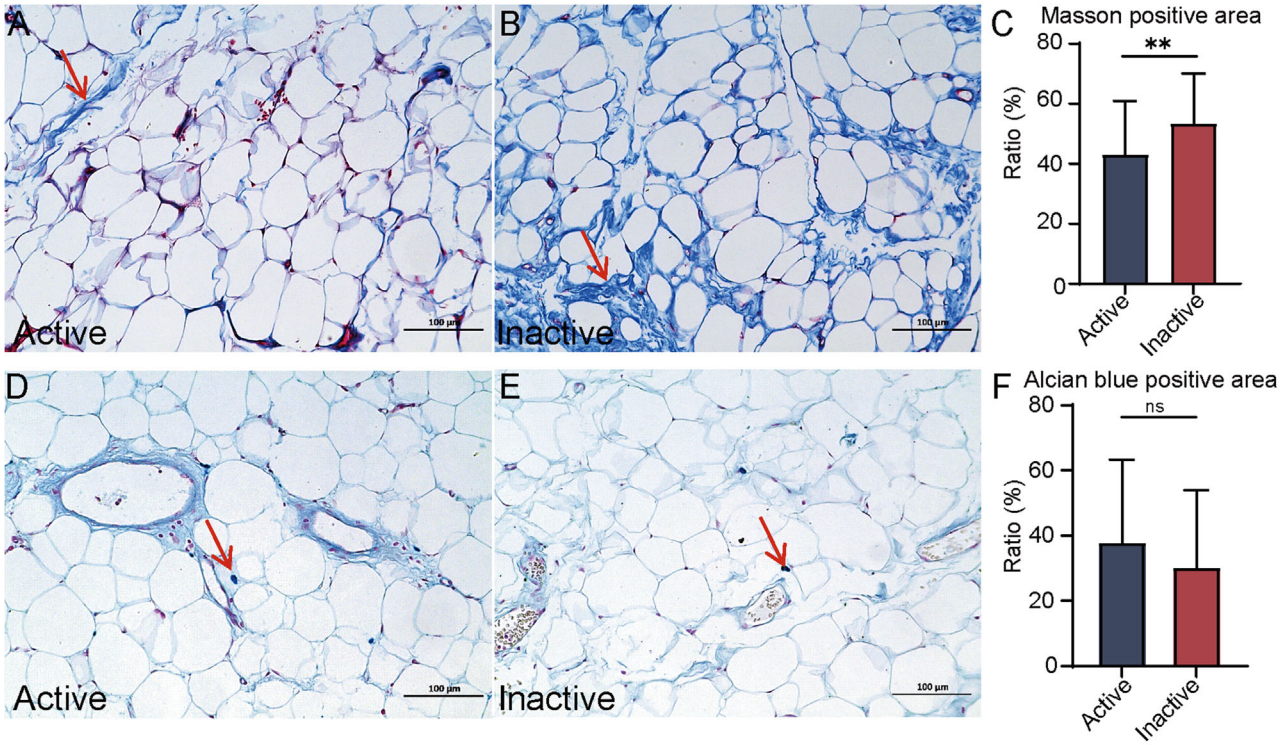

Figure 4. Differences of orbital adipose tissue interstitium between active and inactive subjects. **(A–B)** Representative Masson staining images of orbital adipose/connective tissue in **(A)** active TED subjects and **(B)** inactive TED subjects. **(C)** The corresponding quantitative histogram of Masson positive area ratio between active and inactive TED subjects. (42.9673 ± 17.9052 vs. 53.9348 ± 15.5763; $P < 0.01$). **(D–E)** Representative Alcian blue staining images of orbital adipose/connective tissue in **(D)** active TED subjects and **(E)** inactive TED subjects. **(F)** The corresponding quantitative histogram of Alcian blue–positive area ratio between two groups (0.0379 ± 0.0370 vs. 0.0303 ± 0.0290; $P > 0.05$). The positive staining was indicated by the *red arrows* in **A, B, D,** and **E**. Data were presented as the mean ± SD. ** $P < 0.01$. ns: no significant difference. ($n = 18$ in active group and $n = 15$ in inactive group.)

Table 1. The Correlation Analysis Between Cytokines and Other Pathological Indicators*

Cytokines	T Cells	Th Cells	Tc Cells	Monocytes	B Cells	Adipocyte	Fibrosis	GAGs
IL-16	0.799‡	0.454‡	0.693‡	—	—	—	—	—
CCL18	0.420†	0.471‡	—	0.387†	—	—	—	—
CXCL13	0.601‡	—	0.486‡	—	—	—	—	—
CCL19	0.388†	—	—	—	−0.345†	—	—	—
CCL2	—	—	—	—	0.434†	—	—	—
FGF-13	—	—	—	−0.424†	—	—	0.460‡	—
CXCL14	—	—	—	−0.362†	—	—	0.371†	—
CXCL11	—	—	—	−0.370†	—	—	0.421†	—
IL-10	—	—	—	−0.352†	—	—	0.378†	—
IL-13	—	—	—	−0.383†	—	—	0.360†	—
IL-4	—	—	—	−0.404†	—	—	0.441†	—
IL-11	—	—	—	−0.406†	—	—	—	—
IL-9	—	—	—	−0.357†	—	—	—	—
BDNF	—	—	—	0.418†	—	—	—	—
Serpin E1	—	—	—	0.391†	—	—	—	—
CXCL4	—	—	—	—	—	0.415†	—	—
FGF-23	—	—	—	—	—	—	0.417†	—
CCL26	—	—	—	—	—	—	0.379†	—
TRANCE	—	—	—	—	—	—	0.400†	—
IL-2	—	—	—	—	—	—	0.346†	—
VCAM-1	—	—	—	—	—	—	—	0.373†

T cells, T lymphocytes; Th cells, helper T cells; Tc cells, cytotoxic T cells; GAGs, glycosaminoglycans.
* The results were presented as correlation coefficients and analyzed by Pearson correlation.
† $P < 0.05$.
‡ $P < 0.01$.

viduals.[20,21] This may be attributed to the compressive forces and inflammatory effects on the adipose/connective tissue.[20] As for orbital adipose tissue interstitium, both our study and previous research have revealed more fibrosis in inactive group.[22] Notably, our study demonstrated that the deposition of glycosaminoglycans in the orbital adipose/connective tissue, a hallmark pathological alteration in TED, did not exhibit significant differences between the active and inactive status. It indicated that this pathological alteration may occur independently of the inflammatory process.

Our findings indicated a significant correlation among cytokines, histopathological changes, and clinical characteristics. While correlation does not inherently imply causation, variables that are mutually causal are highly likely to exhibit a correlation. Notably, we identified for the first time that IL-16 and CXCL13 were strongly correlated with T cell infiltra-

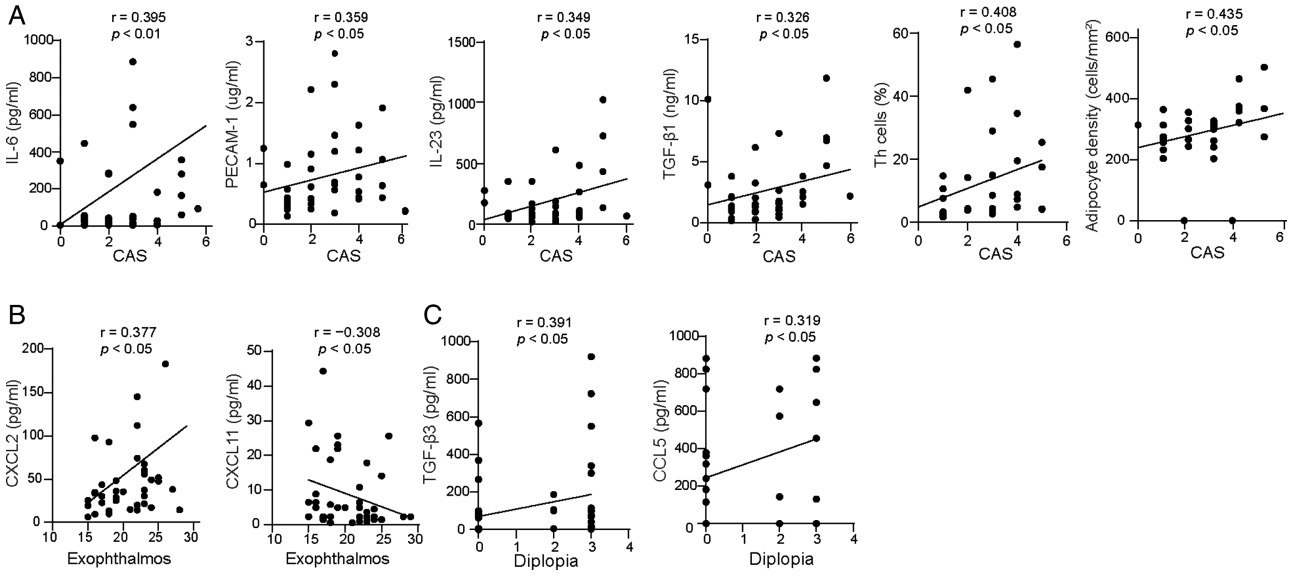

Figure 5. Correlation analysis between pathological changes in orbital adipose/connective tissue and TED clinical characteristics. **(A)** Correlation graphs showing that some pathological changes were significantly positively correlated with CAS, including IL-6, PECAM-1, IL-23, TGF-β1, Th cells, adipocyte density. **(B)** The correlation graphs showing that CXCL2 was significantly positively correlated with exophthalmos, while CXCL11 was significantly negatively correlated with exophthalmos. **(C)** Correlation graphs showing TGF-β3 and CCL5 were significantly positively correlated with diplopia. The *r* value represents the Spearman correlation coefficient, and *P* values were calculated using Spearman correlation tests.

Investigative Ophthalmology & Visual Science

Table 2. The Correlation Analysis Between Pathological Index and Severity

Cytokines	Correlation Coefficient	*P* Value*
VCAM-1	0.405	0.008
CXCL5	0.401	0.008
CXCL13	0.389	0.011
APRIL	0.389	0.011
IL-23	0.379	0.013
PDGF-CC	0.365	0.017
CCL3	0.354	0.021
IL-6	0.356	0.021
PDGF-DD	0.353	0.022
FGF1	0.352	0.022
IL-16	0.346	0.025
CCL2	0.341	0.027
PDGF-AA	0.342	0.027
ICAM-1	0.327	0.034
IL-15	0.310	0.046
Adipocyte density	0.373	0.033

* Analysis by Spearman's rank correlation.

tion in orbital tissues and were associated with the severity of TED. Consistently, previous studies have demonstrated that during the early stages of TED, activated fibroblasts secrete IL-16, which subsequently induces T cell chemotaxis into the orbits, resulting in uncontrolled inflammatory responses.[23,24] Although the specific role of CXCL13 in TED remains unclear, it is known to function as a chemokine in autoimmune diseases, including Graves' disease, by recruiting inflammatory cells such as T cells.[25]

Interestingly, IL-23 and IL-6 were highly expressed in the orbital adipose/connective tissue of active TED subjects and showed a significantly positive correlation with CAS and TED severity, despite not being significantly associated with histopathological changes. IL-23 can initiate tissue inflammation and modulate autoimmune responses upon binding to its receptor (IL-23R).[26] In TED, IL-23 is found to facilitate the differentiation, stabilization, and maturation of Th17 cells. Additionally, IL-23 can stimulate T cells to secrete cytokines and chemokines, which subsequently activate and recruit neutrophils into the orbital tissue of TED.[27] An in vitro experiment has substantiated that the inhibition of IL-23R results in a diminished expression of inflammatory mediators, including IL-6 and IL-8, in orbital fibroblasts, alongside the reduction in glycosaminoglycan synthesis and the manifestation of anti-fibrotic properties.[28]

Regarding IL-6, previous studies employing real-time PCR have demonstrated that the mRNA expression of IL-6 in the orbital adipose/connective tissue of active TED subjects is significantly elevated compared to that in inactive subjects,[29] and this expression is significantly correlated with CAS.[30] Previous research has demonstrated that in TED, IL-6 can enhance the expression of thyroid-stimulating hormone receptor in orbital fibroblasts.[31] IL-6 can also facilitate the differentiation of B cells into plasma cells, which subsequently produce thyroid-stimulating hormone receptor antibodies (TRAb) to activate the inflammatory response.[31] Additionally, other studies have indicated that IL-6 can activate CD86+ M1-like macrophages, which in turn promote fibrosis in both CD34+ and CD34- orbital fibroblasts.[32] Furthermore, pharmacological agents targeting the IL-6 receptor (IL-6R) have been used as an alternative therapeutic intervention for active TED subjects. A randomized controlled trial has substantiated that tocilizumab (humanized monoclonal anti-IL-6R antibody) significantly diminishes the CAS and mitigates the severity of the disease in TED individuals.[33] Collectively, these findings implied that the elevated expression of IL-23 and IL-6 in the orbital adipose/connective tissue of TED subjects may exacerbate inflammatory responses, although these cytokines may not be pivotal in promoting inflammatory cell infiltration and tissue fibrosis.

Our research had identified, for the first time, significant positive correlations between 10 cytokines and fibrosis in the orbital adipose/connective tissue of TED subjects, with FGF-13 exhibiting the strongest correlation. Previous studies have demonstrated that the knockout of the FGF-13 gene in mice inhibits the proliferation and migration of cardiac fibroblasts, thereby significantly reducing interstitial fibrosis. This provides compelling evidence that FGF-13 is a critical factor in the pathogenesis of cardiac fibrosis.[34] Notably, in our study, we displayed a significantly increased fibrosis in the orbital adipose/connective tissue of inactive TED subjects compared to active TED subjects. Fibrosis is known to represent the predominant pathological change in the orbital adipose/connective tissue of inactive TED subjects.[35] We posited that FGF-13 might serve as a promising therapeutic target for anti-fibrotic intervention in subjects with inactive TED.

In conclusion, our study identified significant differences between orbital adipose/connective tissues of active and inactive TED subjects in terms of cytokines, inflammatory cells infiltration, inherent cells and interstitium. We proposed that cytokines, histopathological alterations, and clinical characteristics were interrelated. Although some correlation coefficients in our study were relatively modest, our research established an essential foundation for a comprehensive analysis of the pathological differences between active and inactive TED and their clinical significance.

Acknowledgments

The authors thank Lai Wei and Shuantao Sun for their assistance with this study.

Supported by Military Young Sci-Tech Talents Project; Graduate Student Research Grant From Shandong Second Medical University.

Disclosure: **Y. Li**, None; **J. Tang**, None; **G. Jing**, None; **Y. Li**, None; **R. Ma**, None; **X. Kang**, None; **L. Rong**, None; **W. Liu**, None; **L. Yao**, None; **X. Lv**, None; **A. Deng**, None; **W. Wu**, None; **X. Yang**, None

References

1. Bartalena L, Piantanida E, Gallo D, Lai A, Tanda ML. Epidemiology, natural history, risk factors, and prevention of graves' orbitopathy. *Front Endocrinol*. 2020;11:615993.
2. Bartalena L, Kahaly GJ, Baldeschi L, et al. The 2021 european group on graves' orbitopathy (EUGOGO) clinical practice guidelines for the medical management of graves' orbitopathy. *Eur J Endocrinol*. 2021;185(4):G43–G67.
3. Virakul S, Somparn P, Pisitkun T, et al. Integrative analysis of proteomics and DNA methylation in orbital fibroblasts from graves' ophthalmopathy. *Front Endocrinol*. 2020;11:619989.
4. Martins JR, Furlanetto RP, Oliveira LM, et al. Comparison of practical methods for urinary glycosaminoglycans and serum hyaluronan with clinical activity scores

in patients with graves' ophthalmopathy. *Clin Endocrinol*. 2004;60(6):726–733.
5. Pawlowski P, Reszec J, Eckstein A, et al. Markers of inflammation and fibrosis in the orbital fat/connective tissue of patients with graves' orbitopathy: clinical implications. *Mediators Inflamm*. 2014;2014:412158.
6. Zhang P, Zhu H. Cytokines in thyroid-associated ophthalmopathy. *J Immunol Res*. 2022;2022:2528046.
7. McKeag D, Lane C, Lazarus JH, et al. Clinical features of dysthyroid optic neuropathy: a european group on graves' orbitopathy (EUGOGO) survey. *Br J Ophthalmol*. 2007;91(4):455–458.
8. Rotondo Dottore G, Torregrossa L, Caturegli P, et al. Association of T and B cells infiltrating orbital tissues with clinical features of graves orbitopathy. *JAMA Ophthalmol*. 2018;136(6):613–619.
9. Wong LL, Lee NG, Amarnani D, et al. Orbital angiogenesis and lymphangiogenesis in thyroid eye disease: an analysis of vascular growth factors with clinical correlation. *Ophthalmology*. 2016;123(9):2028–2036.
10. Hai YP, Lee ACH, Frommer L, Diana T, Kahaly GJ. Immunohistochemical analysis of human orbital tissue in graves' orbitopathy. *J Endocrinol Invest*. 2020;43(2):123–137.
11. Bartley GB, Gorman CA. Diagnostic criteria for graves' ophthalmopathy. *Am J Ophthalmol*. 1995;119(6):792–795.
12. Segni M, Bartley GB, Garrity JA, Bergstralh EJ, Gorman CA. Comparability of proptosis measurements by different techniques. *Am J Ophthalmol*. 2002;133(6):813–818.
13. Ameri H, Fenton S. Comparison of unilateral and simultaneous bilateral measurement of the globe position, using the Hertel exophthalmometer. *Ophthal Plast Reconstr Surg*. 2004;20(6):448–451.
14. Bahn RS, Gorman CA. Choice of therapy and criteria for assessing treatment outcome in thyroid-associated ophthalmopathy. *Endocrinol Metab Clin North Am*. 1987;16(2):391–407.
15. Puls M, Beuthner BE, Topci R, et al. Impact of myocardial fibrosis on left ventricular remodelling, recovery, and outcome after transcatheter aortic valve implantation in different haemodynamic subtypes of severe aortic stenosis. *Eur Heart J*. 2020;41(20):1903–1914.
16. dupont NC, Wang K, Wadhwa PD, Culhane JF, Nelson EL. Validation and comparison of luminex multiplex cytokine analysis kits with ELISA: determinations of a panel of nine cytokines in clinical sample culture supernatants. *J Reprod Immunol*. 2005;66(2):175–191.
17. Platchek M, Lu Q, Tran H, Xie W. Comparative analysis of multiple immunoassays for cytokine profiling in drug discovery. *SLAS Discov*. 2020;25(10):1197–1213.
18. Hai YP, Saeed MEM, Ponto KA, et al. A Multicenter, Single-Blind, Case-Control, Immunohistochemical Study of Orbital Tissue in Thyroid Eye Disease. *Thyroid*. 2022;32(12):1547–1558.
19. Eckstein AK, Quadbeck B, Tews S, et al. Thyroid associated ophthalmopathy: evidence for CD4(+) gammadelta T cells; de novo differentiation of RFD7(+) macrophages, but not of RFD1(+) dendritic cells; and loss of gammadelta and alphabeta T cell receptor expression. *Br J Ophthalmol*. 2004;88(6):803–808.
20. Zhang L, Evans A, von Ruhland C, et al. Distinctive features of orbital adipose tissue (OAT) in graves' orbitopathy. *Int J Mol Sci*. 2020;21(23):9145.
21. Regensburg NI, Wiersinga WM, Berendschot TT, Saeed P, Mourits MP. Densities of orbital fat and extraocular muscles in graves orbitopathy patients and controls. *Ophthalmic Plast Reconstr Surg*. 2011;27(4):236–240.
22. Chen MH, Chen MH, Liao SL, Chang TC, Chuang LM. Role of macrophage infiltration in the orbital fat of patients with graves' ophthalmopathy. *Clin Endocrinol*. 2008;69(2):332–337.
23. Lehmann GM, Feldon SE, Smith TJ, Phipps RP. Immune mechanisms in thyroid eye disease. *Thyroid*. 2008;18:959–965.
24. Bahn RS. Current insights into the pathogenesis of Graves'ophthalmopathy. *Horm Metab Res*. 2015;47:773–778.
25. Aust G, Sittig D, Becherer L, et al. The role of CXCR5 and its ligand CXCL13 in the compartmentalization of lymphocytes in thyroids affected by autoimmune thyroid diseases. *Eur J Endocrinol*. 2004;150(2):225–234.
26. Teng MW, Bowman EP, McElwee JJ, et al. IL-12 and IL-23 cytokines: from discovery to targeted therapies for immune-mediated inflammatory diseases. *Nat Med*. 2015;21(7):719–729.
27. Ren Z, Zhang H, Yu H, Zhu X, Lin J. Roles of four targets in the pathogenesis of graves' orbitopathy. *Heliyon*. 2023;9(9):e19250.
28. Pan Y, Wang M, Chen X, et al. Elevated IL-38 inhibits IL-23R expression and IL-17A production in thyroid-associated ophthalmopathy. *Int Immunopharmacol*. 2021;91:107300.
29. Wakelkamp IM, Bakker O, Baldeschi L, Wiersinga WM, Prummel MF. TSH-R expression and cytokine profile in orbital tissue of active vs. inactive graves' ophthalmopathy patients. *Clin Endocrinol*. 2003;58(3):280–287.
30. Jyonouchi SC, Valyasevi RW, Harteneck DA, Dutton CM, Bahn RS. Interleukin-6 stimulates thyrotropin receptor expression in human orbital preadipocyte fibroblasts from patients with graves' ophthalmopathy. *Thyroid*. 2001;11(10):929–934.
31. Bahn RS. Graves' ophthalmopathy. *N Engl J Med*. 2010;362(8):726–738.
32. Lu Y, Wang Y, Wang Y, et al. M1-like macrophages modulate fibrosis and inflammation of orbital fibroblasts in graves' orbitopathy: potential relevance to soluble interleukin-6 receptor. *Thyroid*. 2023;33(3):338–350.
33. Perez-Moreiras JV, Gomez-Reino JJ, Maneiro JR, et al. Efficacy of tocilizumab in patients with moderate-to-severe corticosteroid-resistant graves orbitopathy: a randomized clinical trial. *Am J Ophthalmol*. 2018;195:181–190.
34. Wang C, Wang X, Zhang Y, et al. Inducible Fgf13 ablation alleviates cardiac fibrosis via regulation of microtubule stability. *Acta Biochim Biophys Sin*. 2024;56(12):1802–1812.
35. Dik WA, Virakul S, van Steensel L. Current perspectives on the role of orbital fibroblasts in the pathogenesis of graves' ophthalmopathy. *Exp Eye Res*. 2016;142:83–91.

Investigative Ophthalmology & Visual Science